

SA N097-2225C
SAND-97-2225C

Structure-Property Relationships of Antiferroelectric $\text{Pb}(\text{Zr},\text{Ti})\text{O}_3$ Based Materials:
Hydrostatic Depoling Characteristics CONF-971080--

Bruce Tuttle, Jim Voigt, David Zeuch, Roger Moore, S. Jill Glass, Joseph Michael,
Terry Garino and Walter Olson
Sandia National Laboratories
P.O. Box 5800
Albuquerque, NM 87185 USA

RECEIVED

SEP 18 1997

O.S.T.

Abstract - A novel technique has been developed for the synthesis of homogeneous, weakly agglomerated, highly filterable $\text{Pb}(\text{Zr},\text{Ti})\text{O}_3$ (PZT) powders. PZT 95/5 based ceramics were fabricated from these powders to determine interrelationships among microstructure, dielectric properties and pressure induced ferroelectric (FE) to antiferroelectric (AFE) phase transitions. Initial measurements indicate that microstructure has a substantial effect on hydrostatic depoling characteristics. While smaller grain size materials had higher switching pressures, subtleties in microstructure, which may include entrapped porosity, resulted in a more diffuse depoling characteristic. In addition, greater than 90% dense materials were obtained at process temperatures as low as 900°C. While measured polarizations of the PZT 95/5 ceramics fired at 900°C were only 30% of the values of PZT 95/5 fired at 1300°C, the dielectric constants of the 900°C materials were almost a factor of two higher. Backscattered electron Kikuchi pattern analysis determined that adjacent, nonlinear, irregularly shaped domain structures observed by electron channel imaging were 109° domains.

I. Introduction

$\text{Pb}(\text{Nb},\text{Zr},\text{Ti})\text{O}_3$ (PNZT) 2/95/5 ceramics are the active media for low volume, megawatt explosive power supplies. The basis of operation is the transformation of the PZT 95/5 ceramic from the poled ferroelectric, rhombohedral state to the antiferroelectric, orthorhombic state by application of mechanical pressure. System requirements dictate that the pressure at which the material transforms to the AFE state be very tightly controlled. Specifically, the chemical composition must be controlled to ± 0.05 mole% Ti, to meet

these switching pressure requirements. Another requirement is that substantial current output be obtained. This necessitates excellent chemical uniformity throughout the entire ceramic. The requirements of tight stoichiometric control and a high degree of chemical uniformity are reasons why we have initiated one of the first efforts to combine chemical preparation of powders with added pore formers in the PZT 95/5 system. Effects of grain size, initial PbO stoichiometry, density and porosity on dielectric hysteresis and hydrostatic depoling properties of PZT 95/5 ceramics are described in this paper. Our work represents one of the first attempts to correlate microstructure to hydrostatic depoling behavior.

Strict microstructure control is required in addition to chemical uniformity to meet specifications. This is not surprising, in that the energy differences between AFE and FE phases are highly dependent on mechanical stress, which in turn depends on microstructure. Typically, large grains ($> 20 \mu\text{m}$) are desired for three reasons: (1) to minimize the presence of the AFE phase, (2) to obtain high polarization values and (3) to have a quick, uniform release of charge during pressure transformation. Obviously, the presence of the AFE phase in the microstructure diminishes the remanent polarization and thus current output. Larger grains may also reduce localized stress inhomogeneities and thus minimize localized switching pressure distributions. In addition to the above factors, Storz and Dungan [1,2] showed that addition of pore formers are necessary to prevent high voltage breakdowns at low temperature (-55°C). Their work demonstrated that additions of pore formers, such as, Avicel and Lucite enhance this low temperature performance. While Avicel additions produced acicular pores of approximate 70 μm length and 10 μm width, the Lucite additions resulted in spherical pores of 50 to 100 μm in diameter. Typically, 0.6 wt% of Avicel (approx. 4 volume %) addition and densities in the 90% to 93% of theoretical density range result in the best

DISCLAIMER

**Portions of this document may be illegible
in electronic image products. Images are
produced from the best available original
document.**

DISCLAIMER

This report was prepared as an account of work sponsored by an agency of the United States Government. Neither the United States Government nor any agency thereof, nor any of their employees, make any warranty, express or implied, or assumes any legal liability or responsibility for the accuracy, completeness, or usefulness of any information, apparatus, product, or process disclosed, or represents that its use would not infringe privately owned rights. Reference herein to any specific commercial product, process, or service by trade name, trademark, manufacturer, or otherwise does not necessarily constitute or imply its endorsement, recommendation, or favoring by the United States Government or any agency thereof. The views and opinions of authors expressed herein do not necessarily state or reflect those of the United States Government or any agency thereof.

properties. Materials that were either hot-pressed to greater than 98% density or pressureless sintered to greater than 96% density exhibited 100% failure rate for low temperature (-55°C) explosive tests.

The chemical composition used in this study is $\text{Pb}_{0.991}(\text{Zr}_{0.95}\text{Ti}_{0.05})_{0.982}\text{Nb}_{0.018}\text{O}_3$. Niobium is used to allow operation over a wide temperature range (-55°C to 74°C), enhance poling and increase resistivity. The high to low temperature rhombohedral phase transition occurs at 56°C accompanied by an approximate 0.4% decrease in volume [3]. Slow cooling rates, on the order of 0.1°C/min, are required to prevent larger samples from cracking due to this phase transition. The high temperature rhombohedral phase has space group R3m and the low temperature rhombohedral phase has space group R3c. These phases are distinguished by opposite rotation of the successive oxygen layers along the <111> direction as demonstrated by Dai, Xu and Viehland [4]. No evidence of transformation of the low temperature rhombohedral FE phase to the AFE phase has been observed by Yang [5] by dielectric measurements down to 11K for atmospheric pressure. The pressure / temperature phase diagram by Fritz and Keck [6] indicates that approximately 0.3 GPa hydrostatic pressure is required to transform from the FE to the AFE phase at 25°C for coarse grain, mixed oxide ceramics.

II. Experimental Procedure

PZT powders used in this study were synthesized by an alkoxide / oxalic acid technique. This process minimizes waste and produces a readily filterable co-precipitate compared to other chemical preparation techniques, such as the highly regarded Haertling process [7]. In addition, a very uniform, weakly agglomerated, free flowing powder is obtained. At least 99.95% of all of the original chemical constituents were precipitated as determined by ICP analyses. Zirconium, titanium and niobium butoxides are blended with acetic acid in the initial step of the procedure. The butoxides were chosen to minimize moisture sensitivity and undesirable hydrolysis reactions. A lead acetate/acetic acid mixture is then added to the alkoxides. An oxalic acid / propanol solution is used as the precipitating agent and the wet powders are filtered to assist drying. Oxalic acid / propanol was used to stoichiometrically remove constituents, metal species and minimize agglomeration. 1500 gram lots of PZT 95/5 powder were synthesized for this study.

The precursor powder was pyrolyzed at 400°C, ball milled with ZrO_2 media for 16 hours and then calcined at 775°C for 16 hours. While some powders were processed into small 3 gram samples with no binder or pore former additions, for larger samples, polyvinyl alcohol / polyethylene glycol binder was used. The effects of pore former additions were evaluated by adding 0.6 wt% (approximately 4 volume percent) Avicel particles, which were uniformly incorporated into the powders by ball milling. The powders were uniaxially pressed at 3.5 MPa (5 ksi), and then isopressed at 207 MPa (30 ksi), resulting in green densities on the order of 58% theoretical. Firing was performed using a double alumina crucible technique and mixed oxide PZT 95/5 atmosphere powder. Atmosphere powder configurations were modified depending on sample size. Typically, the fired weight of the specimens corresponded to PbO contents within ± 0.4 mol% of stoichiometry, regardless of the initial PbO stoichiometry of the powders. Compositions with 0 mol%, 1 mol%, 3 mol% and 6 mol% excess PbO were investigated. Firing temperatures from 800°C to 1450°C were investigated, and a baseline treatment of 1345°C for 6 hours was adopted for this study.

Dielectric hysteresis measurements were made using a HP4284A LCR meter. The majority of the ferroelectric measurements were performed using a Radian Technologies RT66A ferroelectric tester with 0.5 sec (2 Hz) driving voltages. While pressure application rates for the hydrostatic depoling measurements varied from 0.69 MPa/sec (100 psi / sec) to 5.26 MPa/sec (765 psi/sec), a pressure application rate of 0.69 MPa/sec was most often used. An approximate 4.5% increase in switching pressure was observed for the 5.26 MPa/sec pressure application rate compared to the 0.69 MPa/sec rate. Our baseline electrode deposition procedure was sputter deposition of 20 nm Cr // 100 nm Au electrodes with an 800°C annealing treatment before deposition. While a JEOL 6400 scanning electron microscope was used for BEKP analysis and electron channel imaging, a Hitachi 4500 FEG-SEM was used for conventional secondary electron imaging. Most imaging was performed on polished samples for which a 0.05 μm colloidal silica abrasive was used for the final polishing step.

III. Results and Discussion

A. Density and Grain Size

The effect of the initial PbO stoichiometry of the PZT 95/5 powders on the fired density as a function of temperature is shown in Figure 1. In our studies, excess PbO additions enhanced low temperature densification of the PZT 95/5 materials, similar to that shown by Hackenberger, Shrout and coworkers [8] for PNZT 2/52/48 materials. Ceramics containing 6 mol% excess PbO had densities greater than 94% of theoretical for a firing temperature of 900°C. The 0% and 3% excess Pb addition samples fired at 1125°C and above in Figure 1, were all processed using improved powder processing and better PbO atmosphere control than for the 6% excess PbO samples. The improved powder processing consisted of a 400°C pyrolysis procedure and ball milling. An example of the improvement is that ceramics with 0% excess PbO fired at 1200°C were only 65% dense using the old techniques, but had extrapolated densities of 88% using the newer procedures. For the improved process, samples fired at 1345°C for 6 hours are 95% to 97% dense, for all three PbO stoichiometries. Close examination of a number of different batches indicated that statistically both densities and grain sizes increased slightly with higher initial PbO content for ceramics fired at 1345°C. Densities for the improved process powder compacts fired at 1125°C ranged from 82% for the 0% excess PbO powders to 96% for the 6% excess PbO powders.

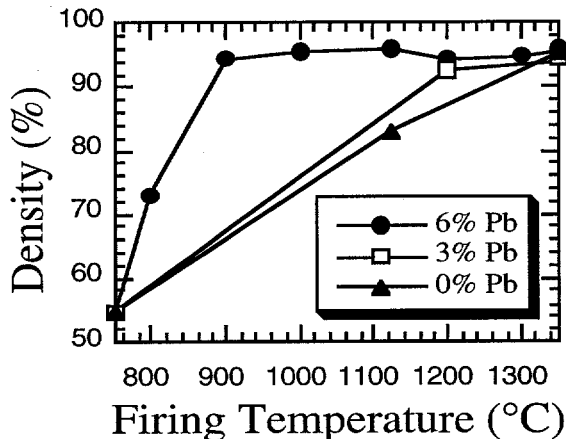


Fig. 1. Density versus firing temperature

B. Dielectric Properties Versus Grain Size

Grain sizes ranging from 0.5 μm to 20 μm were obtained for the chemically prepared PZT 95/5

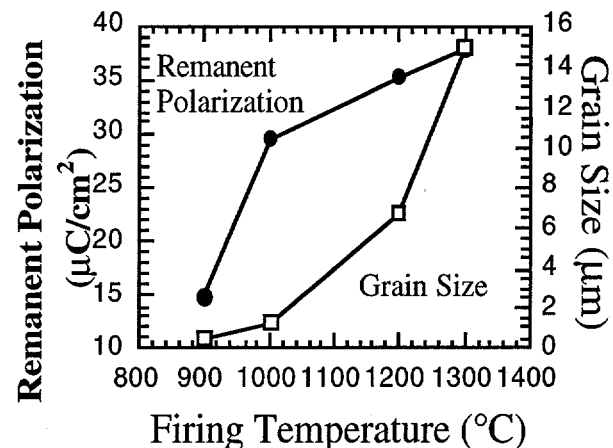


Fig. 2. Polarization and grain size versus firing temperature

ceramics in this study. Grain sizes were calculated using a lineal intercept technique with no three dimensional multiplier. A plot of grain size and remanent polarization versus firing temperature is shown in Figure 2 for samples batched with 6 mol% excess PbO. These 4 samples were all prepared from the same lot of powder and fired at temperatures of 900°C, 1000°C, 1200°C and 1300°C, respectively. A remanent polarization on the order of 38 $\mu\text{C}/\text{cm}^2$ was obtained for the 15 μm grain size sample, while the submicron grain size sample had a remanent polarization of only 15 $\mu\text{C}/\text{cm}^2$. Of potential interest for low fire packaging applications, the 1.5 μm grain size sample had a remanent polarization of 30 $\mu\text{C}/\text{cm}^2$. These grain sizes were calculated using a lineal intercept technique with no three dimensional shape multiplier.

The low field dielectric constants measured at 1 kHz decreased with increasing grain size as shown in Table I. The sample fired at 900°C had a dielectric constant of 511, while the sample fired at 1300°C had a dielectric constant of 281. Dissipation factors were 0.039 and 0.027, respectively. An increase in dielectric constant with decreasing grain size is very common for BaTiO_3 based materials and is attributed to increased internal stress with fine grain size [9]. We have also observed this

enhancement of dielectric constant with decreased grain size for chemically prepared PZT 52/48 based ceramics. While the PbO content after firing is close to stoichiometric for the 1200°C and 1300°C samples, the 900°C sample has the initial 6 mol% excess PbO retained. Because the dielectric constant should decrease with added PbO, the PbO stoichiometry is not a factor in the dielectric constant increase.

TABLE I
Dielectric Properties Versus Grain Size

Dielectric Constant	Remanent Polarization ($\mu\text{C}/\text{cm}^2$)	Grain Size (μm)	d_{33} (pC/Nt)
511	14.8	0.7	29
436	29.6	1.4	61
335	35.2	6.7	69
281	37.9	19.2	67

C. Hydrostatic Depoling Measurements

The hydrostatic pressure required to invoke the FE to AFE phase transition also appears to be grain size dependent. Depoling curves are shown in Figure 3 for two ceramics (Table I) fired at 1200°C and 1300°C for 1.5 hours, respectively. The pressure necessary to invoke the FE to AFE transition increases from 244 MPa to 360 MPa (35.5 to 52.3 ksi) with decreasing grain size. The even finer grain size sample fired at 1000°C had a switching pressure of 365 MPa (53.1 ksi). In addition, the depoling characteristic is more diffuse for the finer grain size ceramics. The increase in distribution of switching pressures with smaller grain size is consistent with an increase in the heterogeneity of localized mechanical stresses. Since higher levels of internal stress would energetically favor the low volume, high pressure AFE phase, an increase rather than a decrease in switching pressure with lower grain size at first seems anomalous. However, inhibition of ferroelastic deformation within the finer grain size sample leading to higher transformation pressures may be a factor that influences the depoling pressure.

We have investigated the effects of additions of Avicel on dielectric and hydrostatic depoling characteristics of PNZT 1.8/95.4/4.6 chemically prepared ceramics. Ceramics from the same batch of powder were fabricated with no pore former and with 0.6 wt% Avicel. The sample with no pore former additions had a density of 97.3% and

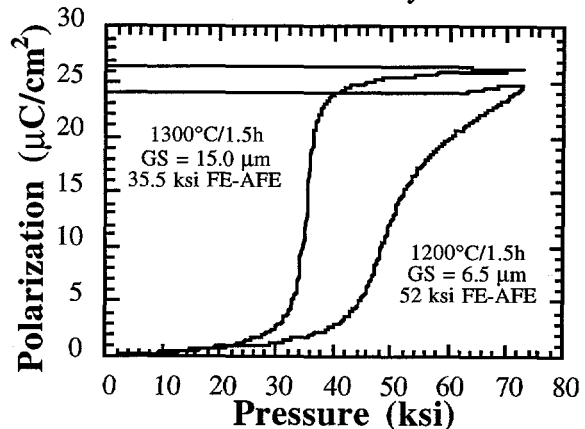


Fig. 3. Hydrostatic depoling characteristics for different grain size ceramics

those with pore former had a density of 92.0%. While samples with pore former had a switching pressure of 263 MPa (38.3 ± 0.3 ksi), samples with no pore former had a switching pressure of 282 MPa (41.0 ± 1.0 ksi). The switching pressure is defined as that pressure for which half the total remanent charge is released. Both samples exhibited a sharp hydrostatic depoling characteristic, similar to that shown in Figure 4 for the ceramic with pore former. The amount of charge released was $37.3 \pm 3.6 \mu\text{C}/\text{cm}^2$ for the material with no pore former and $31.8 \mu\text{C}/\text{cm}^2 \pm 1.3 \mu\text{C}/\text{cm}^2$ for samples with Avicel additions. Remanent polarization values for 30 kV/cm field applications were 34.3 and $37.0 \mu\text{C}/\text{cm}^2$, respectively. Piezoelectric d_{33} coefficients were 73 and 72 pC/Nt , respectively. Thus the pore former slightly affected density and released charge, but other properties only marginally.

Not all chemically prepared samples exhibited sharp depoling characteristics. An example of both a sharp and a more diffuse hydrostatic depoling characteristic are shown in Figure 4. The sharp characteristic is for the previously described 4.6 mol% Ti sample with pore former; whereas the more diffuse characteristic is for a 5.2 mol% Ti sample with no pore former. Some evidence of early charge loss and some slanting of the characteristic

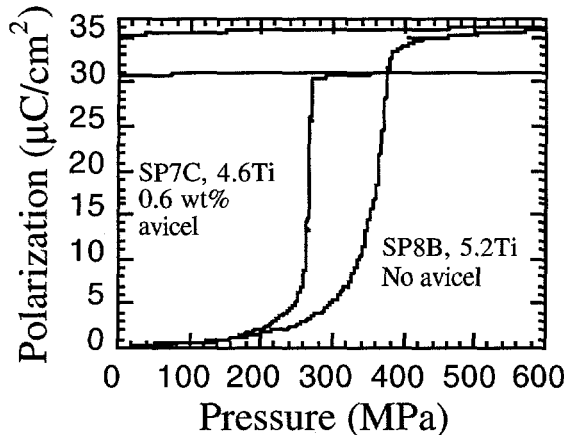


Fig. 4. Hydrostatic depoling curves for chem-prep PZT 95/5 ceramics

shape above 300 MPa during depoling, both of which are detrimental to device performance, are observed for the 5.2 mol% Ti sample. Evidence from several different batches of material indicates that the presence of pore former is not responsible for the differences in depoling characteristic shape.

Systematic studies were performed to see if the electrode preparation procedure was the cause of the differences in depoling behavior. Three different electrode procedures were used for two different batches of chem-prep 95/5 powders. Batch 8B samples contained 5.2 mol% Ti, while Batch 7C samples had 4.6 mol% Ti. The three different electrode techniques for PZT elements whose surfaces were polished with 600 grit SiC abrasive were:

- (1) ultrasonically clean with acetone, anneal ceramic at 800°C for 30 min and sputter deposit Cr//Au.
- (2) sputter deposit Cr// Au, and
- (3) deposit Dupont 7095 Ag frit paste, anneal at 593°C for 20 min .

Little change was observed in hydrostatic depoling characteristics for the 7C materials prepared with different electrode procedures. Hydrostatic transformation pressures of 275, 282 and 290 MPa (40.0, 41.0 and 42.2 ksi) and released polarizations of 35.2, 41.4 and 35.3 $\mu\text{C}/\text{cm}^2$ were obtained for electrode process 1, 2 and 3, respectively. The variation in properties for the samples containing 5.2 mol% Ti was somewhat greater. Hydrostatic transformation pressures of 335, 365, and 358 MPa (48.7, 53.1 and 52.1 ksi) and charge releases of 38.3, 36.3 and 35.3 $\mu\text{C}/\text{cm}^2$

were obtained for the different electrode procedures. The difference in the average depoling pressure for the two different batches is 10.4 ksi, a value which is close to the expected 12 ksi pressure difference based on the 0.6 mol% change in Ti content. The value of change in depoling pressure with Ti content was determined from measurements of large grain, mixed oxide PZT 95/5 ceramics in previous Sandia programs. Further, some of the variation in switching pressure for the 8B samples can be attributed to the slanted depoling characteristic. Conversely, all three 7C samples exhibited sharp depoling characteristics similar to that shown in Figure 4.

The aforementioned differences in hydrostatic depoling characteristic shape thus appear to be inherent in the material itself. Microstructural observations of the two different batches of material indicates that to first order grain size and domain configurations are similar. One identifiable difference is the presence of 1 to 3 μm pores entrapped within the grains of the batch 8B materials. Why these intragranular pores would make a substantial change in hydrostatic depoling characteristic shape, while Avicel derived pores with dimensions on the order of 40 μm by 10 μm do not is not understood at this time. While the entrapped porosity may be a factor in the hydrostatic loop shape difference, it is not the sole cause. Ceramics from other batches of material that had very limited entrapped porosity compared to batch 8B samples also exhibited diffuse characteristics.

D. Determination of Domain Orientations on the Microstructural Level

We have used electron channel imaging in conjunction with backscattered electron Kikuchi pattern analysis [10] to positively identify different domain morphologies of the PZT 95/5 materials. Information from a surface layer 30 nm thick is obtained from the electron channel imaging and BEKP analyses. Thus, the condition of the surface of the sample is critical to the quality of the image obtained. We have used 0.05 μm colloidal silica as a final polish to minimize surface damage. From channel imaging micrographs we have accurately determined grain size and have observed two distinctly different types of domain morphology. The first type of domain configuration identified was the conventional straight, lamellar, 90° type domain configurations often observed in distorted, simple perovskite ferroelectrics. BEKP patterns

were taken of adjacent, domains separated by a straight domain wall on the micron scale. These images were electronically subtracted from one another, indicating a difference of 71° in (111) orientation between the adjacent domains. Thus, these domains corresponded to a perovskite phase of rhombohedral symmetry and the straight, lamellar domains were conventional 90° type domains.

Investigation of the second type of domain morphology, irregularly shaped structures of roughly $2 \mu\text{m}$, was also performed. Initial possibilities as to the origin of these structures included: (1) 180° domains, (2) AFE domain configurations, and (3) 90° type domains. While the irregular domain shapes were very similar to those observed for 180° domains in etched polycrystalline BaTiO_3 and PZT materials, a major difference in diffracted electron intensity for adjacent 180° domains was not expected, BEKP analysis of adjacent domains indicated that the curved domain boundaries separated regions that had (111) directions misoriented by 109° . This result is consistent with these curved structures being 90° type domains of rhombohedral symmetry. While 90° type curved boundaries seem highly unusual, there is previous evidence for this behavior. Randall and coworkers [11] have performed extensive TEM analyses on lead zirconate titanate - lead iron niobate ceramics of rhombohedral symmetry to indicate that curved boundaries were also of the 90° domain type. These domains were not of the same morphology as the domains in our study. Let us caution that this in no way implies that all curved boundaries in etched simple perovskite ferroelectric ceramics are 90° domain type. Indeed, the vast majority of these nonlinear etched structures are 180° type domains, as has been reported by many authors over the last 40 years.

IV. Summary

Chemically prepared PZT 95/5 type ceramics were fabricated and their dielectric properties characterized. Initial studies indicate that pore former additions of approximately 4 volume percent, have only slight impact on dielectric hysteresis behavior, piezoelectric coefficients, and the transformation pressure from the FE to the AFE

state during hydrostatic depoling. Some loss in the charge released during hydrostatic depoling was observed for samples with pore former additions compared to samples with no pore former added. Initial investigations of the effects of microstructure on hydrostatic depoling characteristics indicated that depoling pressures increased with decreasing grain size and that entrapped pores may result in more diffuse hydrostatic depoling characteristics. Backscattered electron Kikuchi pattern analysis was used to positively identify 90° type domains on the microstructural level and to confirm rhombohedral, ferroelectric symmetries of individual grains.

Acknowledgments

Sandia is a multiprogram laboratory, operated by Lockheed Martin Company, for the US Department of Energy under contract DE-AC04AL85000. The authors acknowledge technical contributions and enlightening discussions from Ben Hoover, Pin Yang, Gary Zender, Bonnie McKenzie, Mike Eatough, Mark Rodriguez, Alice Kilgo, Diana Sipola, Jeff Keck, Steve Lockwood, Tim Scofield and Ted Montoya.

REFERENCES

1. L.J. Storz and R.H. Dungan, "A study of the electrical, mechanical and microstructural properties of 95/5 PZT as function of pore former type and concentration," Sandia Report, Sandia National Laboratories, Albuquerque, NM, SAND85-1612 (1985).
2. R.H. Dungan and L.J. Storz, "Relation between chemical, mechanical and electrical properties of Nb_2O_5 modified 95 mol% PbZrO_3 -5 mol% PbTiO_3 ," *J. Amer. Ceram. Soc.*, vol. 68, pp. 530-33 Oct. 1985
3. H. Jaffe, B. Jaffe and W.R. Cook, *Piezoelectric Ceramics*, New York, Academic Press, Inc., 1971, p. 139.
4. X. Dai, Z. Xu and D. Viehland, *J. Amer. Ceram. Soc.*, "Effect of oxygen octahedron rotations on the phase stability, transformational characteristics and polarization behavior in the lead zirconate titanate solid solution series," *J. Amer. Ceram. Soc.*, vol. 78, pp. 2815-23 Nov. 1995.
5. P. Yang, *Internal Sandia Memo*, May 29, 1997.
6. I. Fritz and J. Keck, "Pressure-temperature phase diagrams for several modified lead zirconate ceramics," *J. Phys. Chem. Solids*, vol. 39, pp. 1163-67, (1978).
- 7.. G.H. Haertling and C.E. Land, "Recent improvements in the optical and electrooptic properties of PLZT ceramics," *Ferroelectrics*, vol. 3, pp. 269-80 (1972).
8. W.S. Hackenberger, T.R. Shrout and D.P. Picerell, "Piezoelectric thick films for ultrasonic transducer arrays, *ISHM '96 Proceedings*, pp71-6 (1996).
9. W.R. Buessem, L.E. Cross, and A.K. Goswami, "Phenomenological Theory of High Permittivity in Fine Grained Barium Titanate," *J. Amer. Ceram. Soc.*, vol 49 pp. 33-6 (1966).
10. R.P. Goehner and J. R. Michael, "Phase identification in a scanning electron microscope using Backscattered electron Kikuchi patterns, *J. of Res. of the Nat. Inst. of Standards and Technology*, vol. 101, pp. 301-8 (1996).
11. C.A. Randall, D.J. Barber, and R.W. Whatmore, "Ferroelectric domain configurations in a modified-PZT ceramic," *J. Matls. Sci.*, vol. 22, pp. 925-31 (1987).